Intercalation of Metallocenes in the Layered Transition-Metal Dichalcogenides

Abstract. *Novel intercalation complexes of many of the layered transition-metal dichalcogenides incorporating the metallocenes of cobalt and chromium have been prepared. Evidence is presented indicating a configuration in which the five-membered rings of the metallocene guest are situated perpendicular to the slabs of the dichalcogenide host. In the complexes the metallocenes apparently behave as pseudo-alkali metals, transferring an electron to the chalcogenide.*

The layered transition-metal dichalcogenides are known to incorporate within their two-dimensional van der Waals regions a variety of basic guest species (*1*). The interaction responsible for the formation of these intercalation compounds appears to be charge transfer. The degree of electron transfer from guest to host varies from very little (as is the case with Lewis bases such as the amines) to essentially complete ionization, which holds for the alkali metals.

The metallocenes (Fig. 1) are a class of organometallics composed of a metal ion sandwiched between a pair of cyclopentadienyl rings (ferrocene is the prototype), and they are characterized by low ionization potentials (*2*). Cobaltocene and chromocene—the two members of this series with the lowest ionization potentials (*3*)—can now be added to the list of species (Lewis bases and electropositive metals) that will spontaneously intercalate into the group IV B and group V B dichalcogenides, thus constituting a new set of such inclusion compounds with novel magnetic and electronic properties (*4*).

Table 1. Summary of metallocene intercalations.

Host-guest*	Ratio (weight gain)	*c*-Axis expansion (Å)	Preparation temperature (°C)	Time (days)
TiS_2-$CoCp_2$	0.20	5.55	23°	19
TiS_2-$CrCp_2$	0.30	5.42	100°	3
$TiSe_2$-$CoCp_2$	0.38†	5.52	23°	19
ZrS_2-$CoCp_2$	0.27	5.35	100°	4
HfS_2-$CoCp_2$	0.38†	5.48	100°	5
HfS_2-$CrCp_2$	0.20	5.63	200°	4
$NbSe_2$-$CoCp_2$	0.31	5.53	23°	19
$NbSe_2$-$CrCp_2$	0.20	5.56	100°	7
TaS_2-$CoCp_2$	0.23	5.47	23°	24
TaS_2-$CrCp_2$	0.28	5.52	100°	3
$TaSe_2$-$CoCp_2$	0.42†	5.45	100°	4
$TaSe_2$-$CrCp_2$	0.25	5.57	175°	4
SnS_2-$CoCp_2$	0.29	5.35	100°	4

*Cp, cyclopentadienyl. †Microscopic inspection indicated some occluded solid phase in addition to product.

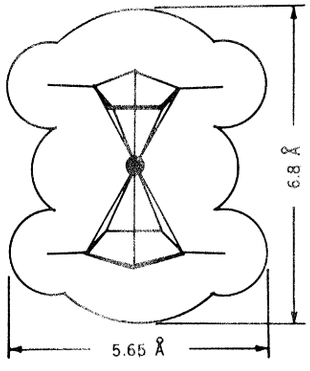

Fig. 1 (top left). Space-filling structure of the metallocenes of the first transition series.

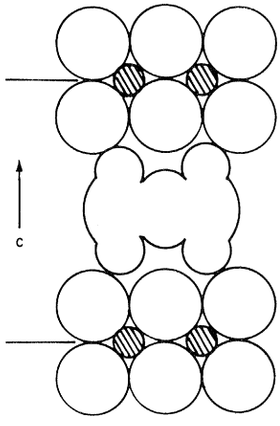

Fig. 2 (top right). Depiction of the intercalation complex. The large circles are the chalogen atoms; the small shaded circles represent the transition elements.

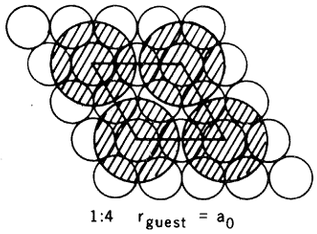

Fig. 3 (bottom right). Projection of the proposed lattice looking down the *c*-direction onto the layer of close-packed chalcogens. The guest is shown as a hatched circle whose diameter is about twice that of the chalcogens (open circles) whose diameters are equivalent to a_0 for the host lattice.

The adducts can be prepared by the simple addition of solutions of the metallocene to the solid host (in an inert atmosphere) under appropriate conditions of temperature and time (see Table 1). The host crystal thus incorporates about 0.25 guest molecule per formula unit. This stoichiometry is verified by the weight gained in the process by the insoluble host and in several cases by elemental analyses. In some cases the weight gained was excessive; this excess was attributed to the fact that it was not possible to completely wash occluded metallocene (or its decomposition products) free from the solid. Optical microscopy revealed some surface contamination.

Powder x-ray diffraction patterns of the products verified complete intercalation (no starting material was present) and also indicated that the structure is most likely one in which the five-membered rings of the metallocene are situated perpendicular to the sheets of the host. The space-filling dimensions of the metallocenes are approximately 6.8 Å along their C_5 axis and 5.65 Å across this axis (Fig. 1). In all of the products described here a dilation of 5.5 ± 0.15 Å in the layer-layer distance of the host was observed (see Table 1), consistent with the structure in Fig. 2. The slight decrease in the observed expansion from the value of 5.65 Å can be attributed to the fitting of the guest within the close-packed chalcogen layers, and possibly also to a small contraction resulting from the ionization that probably accompanies the inclusion:

$$0.25\ MCp_2 + TX_2 \rightarrow (MCp_2)^{\oplus}_{0.25}\,TX_2^{1/4\ominus}$$

where MCp_2 is the metallocene and TX_2 is the layered host.

That the guest is ionized in the product is corroborated by the magnetic properties observed (*4*) and is deduced from the fact that the ionization potential seems to be the critical factor in the reactivity of the guests. Thus there is a net release of energy resulting from the summation of the ionization potential of the metallocene, the electron affinity of the host, and the electrostatic crystal energy of the charge-separated complex which renders the product energetically favorable only for cobalto-

cene and chromocene among the "pure" metallocenes of the first row of the first transition series.

If in the intercalation compound we visualize the metallocenes as spinning freely about an axis parallel to the *c*-direction, they can be approximated as cylinders with a diameter of about 6.6 to 6.8 Å (and heights of about 5.5 Å). This value for the circle swept out by a spinning guest is very nearly equal to twice the a_0 distance of the host lattices (effectively the diameter of the chalcogen). Therefore, the experimentally implied stoichiometry of the products can be accounted for simply by projecting on the close-packed chalcogen layer circles having radii *r* equal to the chalcogen diameters (see Fig. 3). Since there are two chalcogen layers per metallocene layer, one predicts a value of 4 : 1 for the host-to-guest ratio. The presumed motion of this model has been verified by broad line nuclear magnetic resonance experiments which will be reported elsewhere (*5*). Details of the structures are presently being investigated and will be reported later.

MARTIN B. DINES
Exxon Research and Engineering Company, Linden, New Jersey 07036

References and Notes

1. F. R. Gamble, J. H. Osiecki, M. Cais, R. Pisharody, F. J. DiSalvo, T. H. Geballe, *Science* **174**, 493 (1971).
2. G. E. Coates, M. L. H. Green, K. Wade, *Organometallic Compounds* (Methuen, London, ed. 3, 1968), vol. 2, chap. 4.
3. M. R. Litzow and T. R. Spalding, *Mass Spectrometry of Inorganic and Organometallic Compounds* (Elsevier, New York, 1973), p. 511.
4. An investigation of the magnetic and transport properties of these compounds will be presented elsewhere (A. H. Thompson and F. R. Gamble, in preparation).
5. B. G. Silbernagel, in preparation.

13 December 1974

Ganymede: Observations by Radar

Abstract. *Radar cross-section measurements indicate that Ganymede scatters to Earth 12 percent of the power expected from a conducting sphere of the same size and distance. This compares with 8 percent for Mars, 12 percent for Venus, 6 percent for Mercury, and about 8 percent for the asteroid Toro. Furthermore, Ganymede is considerably rougher (to the scale of the wavelength used, 12.6 centimeters) than Mars, Venus, or Mercury. Roughness is made evident in this experiment by the presence of echoes away from the center of the disk. A perfectly smooth target would reflect only a glint from the center, whereas a very rough target would reflect power from over the entire disk.*

We have made radar observations of Ganymede, Jupiter's largest satellite, on six nights in late August 1974. The radar that we used for this experiment is located at the Goldstone Tracking Station in the Mojave Desert and is operated for the National Aeronautics and Space Administration by the Jet Propulsion Laboratory. We transmitted a 400-kw, monochromatic beam of microwaves to Ganymede. After the round trip time-of-flight (1 hour and 7 minutes), we switched the antenna to receive and collect power spectrograms of the very weak echoes for an equal time. We could complete three to four such send-receive cycles in each of the six nights during which we collected data.

During the send part of the cycles, the transmitter frequency was switched alternately to +540 hertz and −540 hertz on a 60-second cycle. The phase of this cycle was carefully noted for use one round trip time later. This was done to enable us to remove from the spectrograms the background noise level (which was some 800 times the signal level). All of the spectra for which the signals were low in frequency were subtracted from those for which the signals were high. This resulted in an inverted signal spectrum displaced to the left 540 hertz, followed by the normal spectrum displaced equally to the right. The resultant base line was very flat and free from effects of the system background.

We improved the signal-to-noise ratio by combining the two halves of each spectrum by the operation of shift (1080 hertz) and subtract. This final processing yields the normal spectrum but also results in a half-amplitude, inverted spectrum on either side of the normal one.

Figure 1 is an example of the effects of the processing. It is a theoretical spectrogram, computed for the rough surface which best fits our data. The bracket along the abscissa marks the maximum Doppler shift, 854 hertz, between the approaching and receding limbs of Ganymede, the shift having been computed from the radius (2635 km) as determined by Carlson *et al.* (*1*) and a rotation period of 7.155 days.

Figure 2 shows a set of received spectrograms, each averaged over one night. Although these signals are very noisy, the telltale signature of Fig. 1 can be seen in each. The error bars in Fig. 2 represent ± the standard deviation and are computed for the specific processing system. When the area under each spectrum is calculated, the center frequency being estimated from the average of all the spectra, the total signal power is obtained. The powers are corrected for distance, antenna gain, system noise temperature, and transmitter power, and are converted to radar cross section.

These results are plotted in Fig. 3, expressed as the percentage of the cross section as compared to that of a perfectly conducting sphere. The abscissa is the orbital phase angle. Since Ganymede is in synchronous rotation (*2*) about Jupiter, the part viewed from Earth changes with the phase angle. The variations in the radar cross section in Fig. 3 do not appear to be statistically significant, however, as in Fig. 2, the error bars are calculated.

The spectrograms are computed over a bandwidth of 4 khz and with a resolution of 187 hertz. The signal, of course, is expected to be in the center. Because of the orbital motions of Ganymede and Earth and the rotation of Earth, there is a Doppler shift in the echo of hundreds of kilohertz. A precomputed ephemeris was used to automatically tune the radar receiver so that the echo would be centered in the passband. The ephemeris must be accurate enough to prevent significant frequency drift over each night of observation.

The ephemeris we used, computed by P. A. Laing of the Jet Propulsion Laboratory, had such accuracy that we could average the data over all six nights and thereby realize a much needed improvement of $\sqrt{6}$ in the signal-to-noise ratio.

Figure 4 is the average spectrogram. It is the principal result of our measurements and is admittedly noisy. It represents, however, a clear radar detection of Ganymede

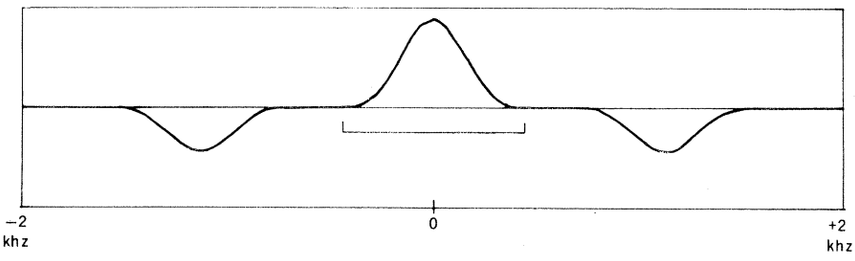

Fig. 1. Calculated spectrogram for the Ganymede surface based on the assumed backscattering function $F(\theta) = \cos^{10}\theta$, where θ is the angle of incidence. The instrumental response is included.